

Atomic Force Microscopy and FT-IR Spectroscopy Investigations of Human Heart Valves

M. JASTRZEBSKA¹, J. ZALEWSKA-REJDAK¹, I. MRÓZ², B. BARWINSKI²,
R. WRZALIK³, A. KOCOT³ AND J. NOŻYNSKI⁴

¹ *Department of Biophysics, Faculty of Pharmacy, Medical University of Silesia, Sosnowiec, Poland*

² *Institute of Experimental Physics, University of Wrocław, Plac Maxa Borna 9, 50–204 Wrocław, Poland*

³ *Department of Biophysics and Molecular Physics, Institute of Physics, University of Silesia, Uniwersytecka 4, 40–007 Katowice, Poland*

⁴ *Department of Histology and Embryology, Medical University of Silesia, Jordana 17, 41–807 Zabrze, Poland*

Abstract. Human aortic, mitral, tricuspid and pulmonary heart valves were investigated by the contact mode atomic force microscopy (AFM) in air, and using FT-IR spectroscopy in the frequency range 950–4000 cm⁻¹. Heart valves were collected *post mortem* from 65–78 years old patients who died from non-cardiac diseases.

All of the examined valves showed considerable heterogeneity in the surface topography of collagen fibrils as well as in their organization on the tissue surface. The AFM images revealed areas with significantly different spatial organization of the collagen fibril bundles. We observed zones with multidirectional, stacked collagen fibrils as well as areas of thin fibrils packed regularly, densely and “in phase”. The majority of the collagen fibrils reproduced the typical transverse D-banding pattern, with the band interval varying in rather wide range of 70–90 nm. Using AFM imaging, objects that correspond to some pathological states of heart valves at their early stages, i.e. some forms of mineral deposits, were observed.

The FT-IR spectra allowed us to recognize main components, i.e. collagen and elastin, in different layers (ventricularis, fibrosa) of the valve leaflets as well as they gave also support for the presence of mineral deposits on the valve surface.

The presented results showed, that the AFM imaging and FT-IR spectroscopy can be applied as a complementary methods for structural characterization of heart valves at the molecular and supramolecular levels.

Correspondence to: Maria Jastrzebska, Department of Biophysics, Faculty of Pharmacy, Medical University of Silesia, Ostrogórska 30, 41–200 Sosnowiec, Poland
E-mail: maja@slam.katowice.pl

Key words: FT-IR spectroscopy — Atomic force microscopy — Heart valves — Collagen fibrils — Supramolecular structure

Introduction

Structural investigations of the heart valve tissue hold a great promise for improved treatment of valve diseases as well as for technological progress in preparation of valve bioprostheses. Significant advances have been made in the early 1990s, however, the subject remains in its infancy and many problems remain to be resolved (Shoen and Levy 1999; Yacoub and Cohn 2004). Primary among these is our limited understanding of the normal heart valve structure and function. A thorough knowledge of molecular structure of heart valve tissue seems to be an essential prerequisite to construct the desired tissue-engineered valve prostheses.

According to the basic anatomy, heart valve leaflet consists of a valve interstitial matrix enveloped by a continuous monolayer of the valvar endocardial cells (Stevens and Lowe 1997). The principal components of the valve extracellular matrix are the fibrous macromolecules collagen and elastin, proteoglycans and glycoproteins. According to Kunzelman et al. (1993), content of collagen, elastin and proteoglycans are equal to about 60, 10 and 20% of the dry weight of the valve, respectively. The collagen component is predominantly type I and III (74 and 24%, respectively). Collagen fibre bundles appear to be surrounded by elastin fibrils. The glycosaminoglycans form a highly hydrated gel-like ground substance in which other matrix molecules are located.

According to literature data (Hurle et al. 1985; Datta et al. 1999; Mirzaie et al. 2002), most of the structural investigations of the human heart valves and heart valve bioprostheses were performed by scanning electron microscopy and light microscopy, therefore different fixation and staining procedures were used. Fixation with glutaraldehyde belongs to the standard procedures. However, atomic force microscopy (AFM) investigations showed that chemical stabilization with glutaraldehyde caused considerable changes in the surface topography of collagen fibrils in pericardium tissue (Jastrzebska et al. 2005).

The AFM represents a novel and increasingly important method for noninvasive examination of the surfaces of different biological materials under slightly altered physiological conditions. AFM enables morphological studies revealing nanometer-scale details of biological objects. Unlike electron microscopes, samples do not need to be stained, coated, dehydrated or frozen (Jena and Hörber 2002).

The purpose of this study was to characterize the supramolecular structure of four human heart valves: aortic, pulmonary, tricuspid and mitral, using AFM imaging. The analysis of the AFM images was focused on the surface topography of collagen fibrils as well as on their spatial organization on the tissue surface. The Fourier transform infrared (FT-IR) spectroscopy allowed us to investigate molecular structure of the main components of the valve tissue.

Materials and Methods

Materials

Aortic, mitral, tricuspid and pulmonary heart valves were collected *post mortem* from four patients, 65–78 years old who died from non-cardiac diseases, according to the protocol of multiple organ procurement from cadaver donors (Rosenthal et al. 1983). Briefly, during first 12 h after the death, the skin of the cadaver was disinfected using betadine alcoholic solution. Then the sterile disposable blades were used for the skin and sternocostal cartilages dissection. After opening the pericardial cavity, the heart was excised using sterile scissors. Then the heart was immersed in sterile physiologic saline and transported to sterile room for preparation of valve leaflets. The preparative procedure was conducted under the saline, also in sterile conditions. The excised leaflets were placed in phosphate buffered saline buffer, pH 7.4 and kept at 4°C. The central part of each valve was excised and subjected to AFM and FT-IR spectroscopic measurements.

Measurements presented in the paper were approved by the Human Experimentation Committee of the Medical University of Silesia, Poland.

Collagen type I isolated from bovine Achilles tendon and elastin isolated from bovine neck ligament were purchased from Sigma.

FT-IR spectroscopy

The IR spectra were taken using FT-IR-6000 Bio-Rad spectrometer equipped with cooled DTGS detector and KBr beamsplitter. The KBr pellets of collagen and elastin were prepared with 1 mg of protein *per* 100 mg of KBr. For the tissue samples, the IR reflecting spectra transformed to the absorption spectra have been recorded. The spectra were collected with spectral resolution of 1 cm⁻¹, in the range of 950–4000 cm⁻¹. For all samples, spectral intensity was normalized using the CH vibrational mode at 1447 cm⁻¹ as an internal standard. Measurement was done at room temperature.

AFM measurements

AFM imaging was performed using the NanoScope E (Digital Instruments, USA) working in the contact mode. The microscope was equipped with OTR8 probe (Veeco NanoProbeTM). The spring constant of the used V-shaped cantilever was 0.15 N/m while its length was 200 μm. The applied constant forces were about 10 nN. The maximum size of images in both X and Y horizontal directions was 13 μm, the maximum height (Z-limit) was 3.8 μm. A single measurement (one frame 512 × 512 pixels) lasted about 300 s. Two standard AFM signals, height and deflection, were registered. The samples were rather soft therefore the images were obtained with lateral and height resolution of about 10 and 1 nm, respectively. The software package WSxM (Nanotec Electronica, Spain) was used for image processing.

The valves were divided into small rectangles (of about 5 × 10 mm). Then the fragments were rinsed with distilled water and placed onto clean glass microscope slides. The measurements were performed in air. To obtain stable images,

the samples had to be gently dried on air, at room temperature, until the excess of water had evaporated from the sample surface. The drying process lasted about 30 min. Longer drying did not cause considerable changes in the surface topography. The results presented in the earlier paper by Jastrzebska et al. (2005) indicate that similar (short and gentle), drying procedures do not affect significantly the surface topography of pericardium tissue, including the D-spacing pattern of collagen fibrils and the spatial arrangement of the fibrils within the pericardium tissue. After short drying on air at room temperature, collagen fibrils, which were imaged on tissue surface, were still in a hydrated state. Therefore, the properties of collagen fibrils in the investigated valves are expected to be close to the normal, native state.

Results and Discussion

AFM images

Fig. 1 shows height (a and c) and deflection (b and d) images of human pulmonary and aortic valves, respectively.

In our experiment, the endothelial layer has been partially lost owing to short time drying of the sample before measurement. Endothelium is the most vulnerable component of the valve leaflets. Partial missing of the endothelium has exposed bottom fibrous layer, however, some remnants of the endothelial layer can be present on the sample surface. Fig. 1 (b and d) shows collagen fibrils with the characteristic transverse D-banding pattern consisting of subsequent grooves and ridges. Such banding pattern, varying in the range 60–70 nm, was observed earlier using AFM and scanning tunneling microscopy methods for studying surface topography of collagen fibrils isolated from different sources (Baselt et al. 1993; Revenko et al. 1994). In our paper we present collagen fibrils in their natural environment of the valve tissue. Fig. 1 (e and f) shows axial profiles, which describe the surface topography of the part of collagen fibrils taken along the marked lines. The mean distances between the neighbouring grooves for pulmonary and aortic valves are equal to 65 ± 6 nm and 58 ± 6 nm, respectively. The difference in height between the grooves and ridges has been found slightly higher for aortic (~ 2 – 4 nm) than for pulmonary (~ 1 – 2 nm). For the aortic valve, the collagen fibril bundles are thicker and arranged in more corrugated manner than for the pulmonary valve. Collagen fibril bundles are surrounded by the elastin fibrils, which are much thinner than collagen fibrils and arranged in a branching pattern (Stevens and Lowe 1997). They are not seen in the images presented in this paper.

Fig. 2 shows height (a and c) and deflection (b and d) images of the mitral valve at two different magnifications. In Fig. 2b one can observe very thick collagen fibril bundle, which may correspond to the insertion of the cords into the valve. One of the characteristic components of the mitral valve is a set of cords connected to the valve (Stevens and Lowe 1997). Valve surface reveals crimp structure, which can correspond to the attached cords. Cords are different in size, shape, orientation and mode of insertion into the valve. Fig. 2e presents an axial profile of the collagen

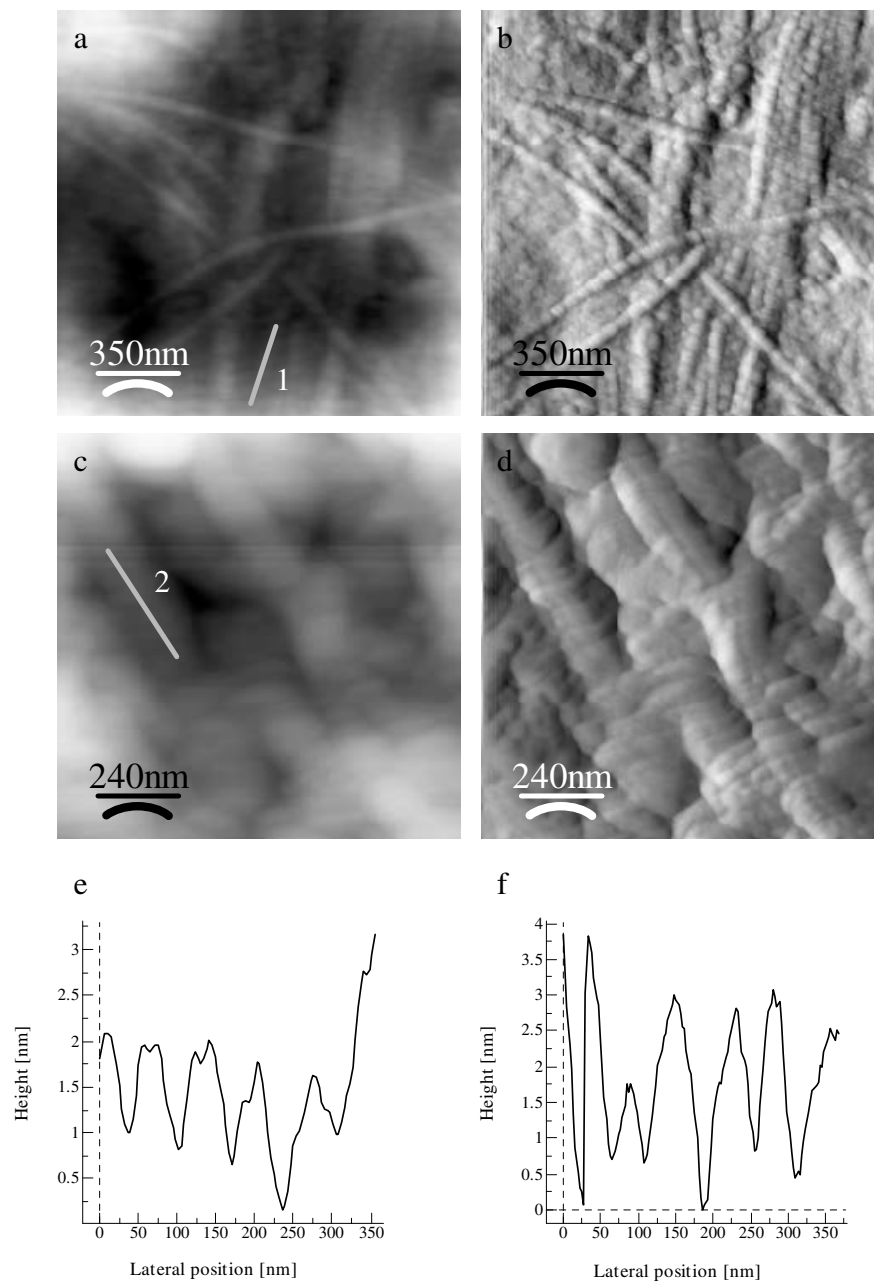


Figure 1. AFM height (a and c) and deflection (b and d) images of the human pulmonary and aortic valves, respectively. The images span the fields $1.8 \times 1.8 \mu\text{m}$ (pulmonary) and $1.2 \times 1.2 \mu\text{m}$ (aortic). The curves (e and f) show axial profiles of the collagen fibrils taken along the marked lines: for pulmonary (line 1) and for aortic (line 2) valves, respectively.

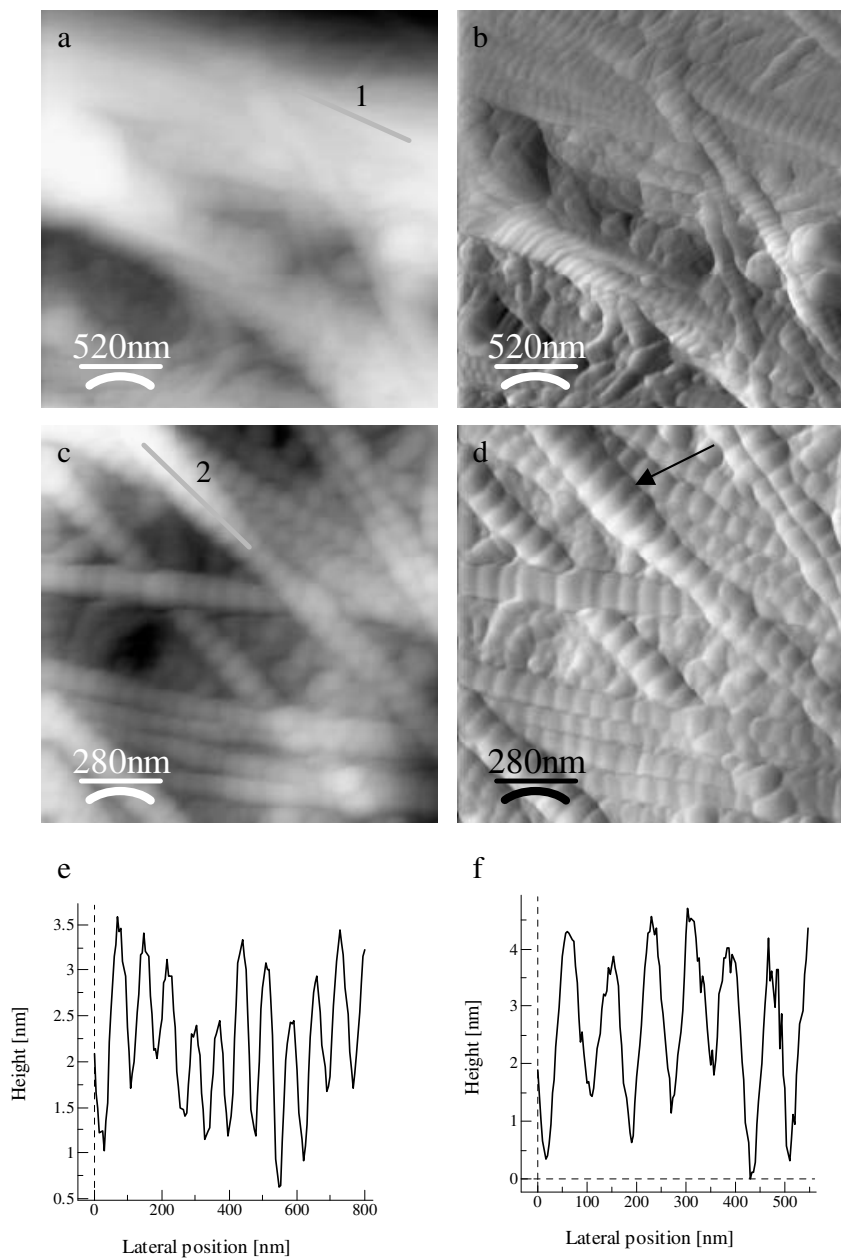


Figure 2. AFM height (a and c) and deflection (b and d) images of the human mitral valve at two different magnifications: $2.6 \times 2.6 \mu\text{m}$ and $1.4 \times 1.4 \mu\text{m}$. The observed thick fibrillar bundle in (b) corresponds probably to the cords, which are inserted into the valve. The curves (e and f) show axial profiles taken along the lines 1 and 2 on the fibril surface, respectively. Arrow shows local swelling on the fibril surface.

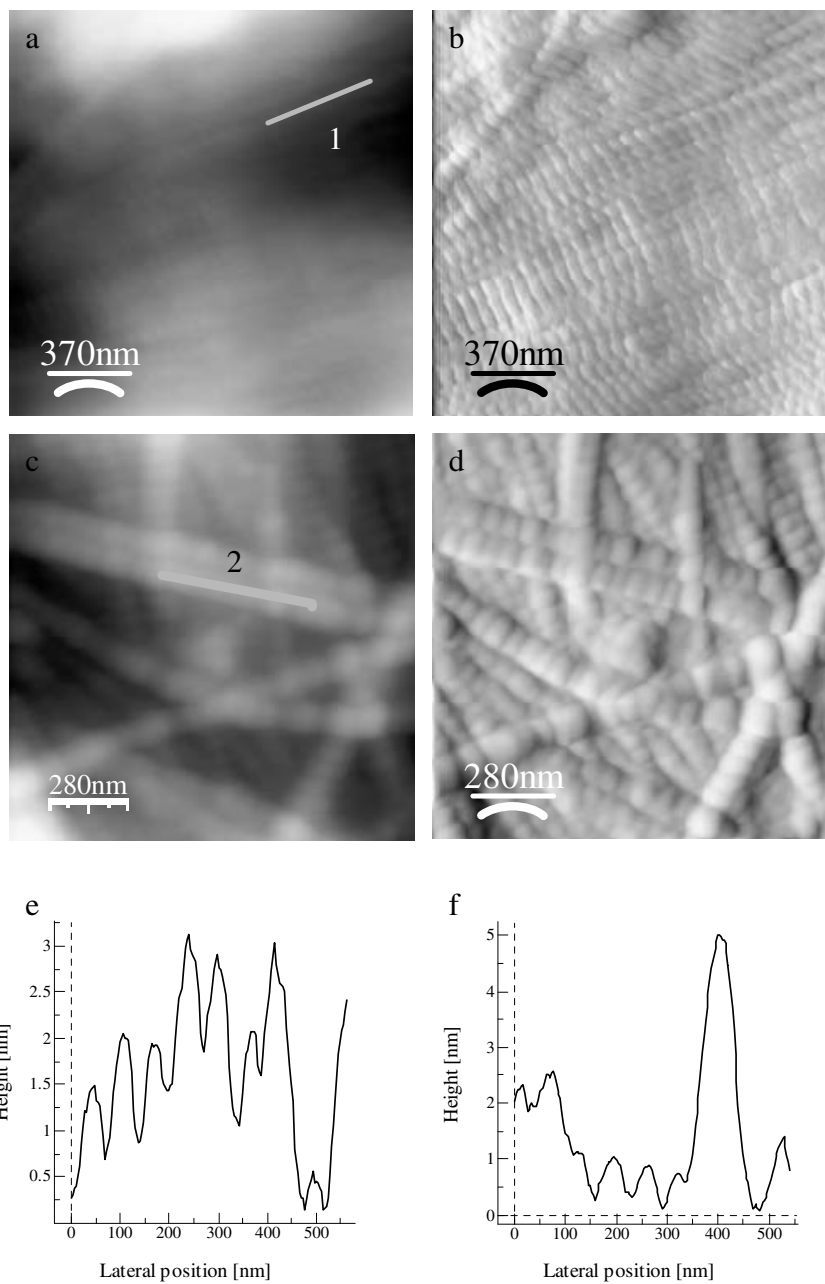


Figure 3. AFM height (a and c) and deflection (b and d) images of human tricuspid valve showing two different modes of collagen fibrils packing, i.e. dense and “in phase” (b, $1.8 \times 1.8 \mu\text{m}$) and loose (d, $1.4 \times 1.4 \mu\text{m}$). The curves (e and f) show profiles taken along the marked lines 1 and 2, respectively.

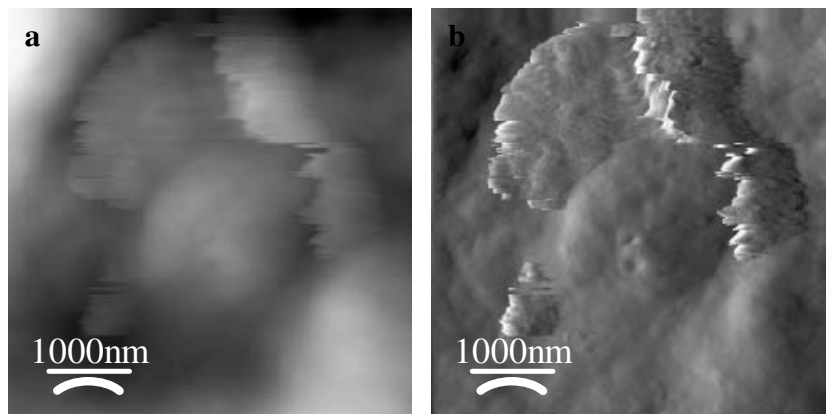


Figure 4. AFM height (a) and deflection (b) images of human pulmonary valve ($5 \times 5 \mu\text{m}$). Different forms of mineral deposits are shown.

fibril located in a relatively smooth area of the valve imaged in Fig. 2b (the right upper part of the image). The mean distance of the D-period is equal to 74 ± 8 nm. Fig. 2d shows collagen fibrils on the surface of the mitral valve at higher magnification. Some fibrils exhibit areas with local swellings. An axial profile taken along the fibril swelling (Fig. 2f) shows D-period equal to about 80 nm.

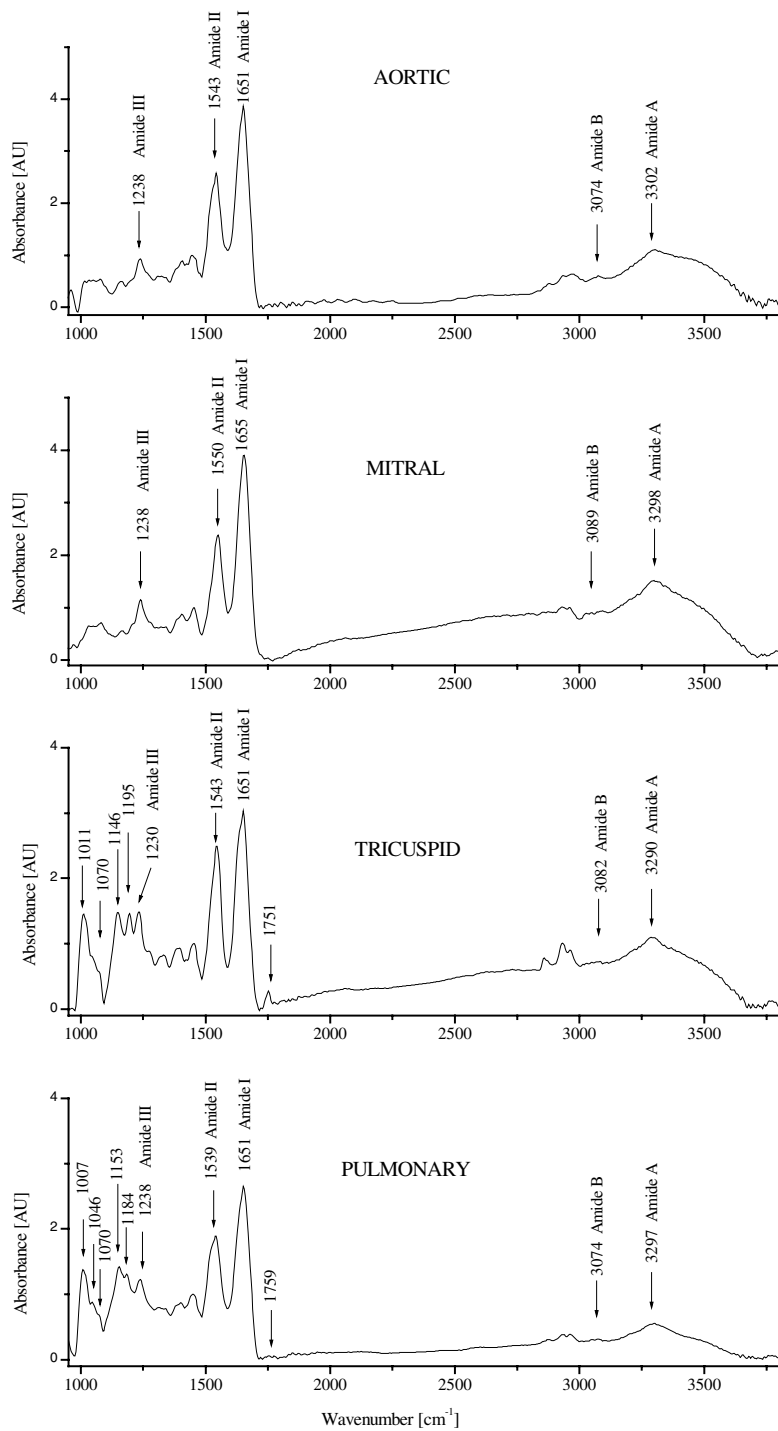
The AFM images have also revealed a different local architecture of collagen fibrils on the valve surface. Fig. 3 shows height (a and c) and deflection (b and d) images for the tricuspid valve. In the most cases, one can observe zones with multidirectional fibril arrangement, as it is shown in Fig. 3d. However, there are also areas with extremely dense packing of parallel thin collagen fibrils, as shown in Fig. 3b. The characteristic feature of such dense packing is, that collagen fibrils are aligned with the same groove/ridge phase. The observed alignment “in phase” can imply some form of intermolecular coupling, which requires further studies for explanation. Curves in Fig. 3 (e and f) show axial profiles taken along the marked lines on the collagen fibril surfaces. The mean value of the characteristic repeating D-distance for loosely arranged fibrils reaches 80 ± 6 nm (Fig. 3f), whereas fibrils with dense packing and alignment “in phase” reveal lower D-distance, 63 ± 6 nm (Fig. 3e). For future analyses, it seems to be important to test mechanical properties of the composition of collagen fibrils with dense packing and aligned “in phase”.

Fig. 4 shows height and deflection images of the pulmonary valve with an object, which can be classified as a mineral deposit. The deposits show the porous structure and they are covered partially by the endothelial layer. According to Jorge-Herrero et al. (2005), such deposits can correspond to the “intrinsic” mineralization, which begins deep within the substance of the valve. Difficulties in imaging that manifest themselves as disfigured parts of Fig. 4 may suggest that

Table 1. Peak frequencies of the selected bands of the FT-IR spectra for human heart valves: aortic, mitral, tricuspid and pulmonary, and for collagen and elastin

Bands	Aortic (cm^{-1})	Mitral (cm^{-1})	Tricuspid (cm^{-1})	Pulmonary (cm^{-1})	Collagen (cm^{-1})	Elastin (cm^{-1})	
CH (b)			1011				Ignjatovic et al. 2001 Chang and Tananka 2002 Low-Ying et al. 2002 Sockalingum et al. 2002
COH (b)			1070	1046			
of			1146	1070			
carbohydrates;				1153			
phosphate group				1184			
PO_4^{3-} (s)		1195					
Amide III							
N-H (b)	1238	1238	1230	1238	1239	1237	
Amide II							
C-N (s),	1543		1543	1539		1535	
N-H (b)		1550			1551		
Amide I	1651		1651	1651			
C=O (s)		1655			1654	1655	Twardowski and Anzenbacher 1994 Singh 2000
C=O ester			1751				
				1759			
Amide B	3074			3074		3072	
C-H (s)		3089	3082		3082		
Amide A			3290				
N-H (s)	3302	3298		3297		3310	

(s), stretching; (b), bending.



the deposits (or some fragments of the deposits) are fragile or they are loosely adhered to the valve surface.

FT-IR spectra

Fig. 5 shows FT-IR spectra of the four human heart valves: aortic, mitral, tricuspid and pulmonary, recorded in the frequency range $950\text{--}4000\text{ cm}^{-1}$. The strongest absorption bands in the spectra are those of the amide peptide group CONH, which is a repeat unit of the polypeptide chain backbone. Generally, amide I band originates from the (C=O) stretching vibrations coupled to (N-H) bending vibrations. The amide II band arises from the (N-H) bending vibrations coupled to (C-N) stretching vibrations. The amide III originates from the (N-H) bending vibrations (Twardowski and Anzenbacher 1994; Singh 2000). Positions of all amide bands are collected in Table 1. The broad band in the range ($3000\text{--}3600\text{ cm}^{-1}$) includes following peaks: OH stretching vibrations, amide A (N-H stretching) and amide B (C-H stretching) vibrations (Table 1). In Fig. 6, the FT-IR spectra of collagen and elastin are presented. As it is shown in Table 1, there are no substantial differences in positions of amide III band for collagen, elastin and for all heart valves, except the tricuspid, which is shifted to lower frequencies (1230 cm^{-1}).

Peak frequencies of the amide II and amide B for elastin ($1535, 3072\text{ cm}^{-1}$) are shifted to lower values in comparison to the frequencies for collagen ($1551, 3082\text{ cm}^{-1}$). Similar shift to lower frequencies can be observed for pulmonary valve ($1539, 3074\text{ cm}^{-1}$) in comparison to the mitral valve ($1550, 3089\text{ cm}^{-1}$). The observed shift in peak positions can prove, that there is the higher content of elastin in pulmonary than in the mitral valves. As the spectra were measured in the reflecting mode, the higher elastin content corresponds to the ventricularis layer of the pulmonary valve. The ventricularis layer covers the pulmonary valve from the inflow side and is abundant in elastin fibrils.

For the mitral valve, the positions of the amide II and amide B are very similar to those in the collagen spectrum (Table 1), giving a spectral evidence for collagen as a dominant component. The dominant content of collagen corresponds to the fibrosa layer of the mitral valve. The fibrosa layer lies generally towards the outflow surface of the valve.

For aortic and tricuspid valves, not so close coincidence in peak positions compared to collagen and elastin has been found.

In Fig. 5, one can also observe two pronounced absorption bands for tricuspid and pulmonary valves, first in the range $1000\text{--}1070\text{ cm}^{-1}$ and the second in the range $1100\text{--}1200\text{ cm}^{-1}$. According to Ignjatović et al. (2001) and Chang and Tananka (2002), the bands with the maxima in the range $1000\text{--}1200\text{ cm}^{-1}$ are attributed to the vibrations of phosphate groups from the hydroxyapatite. Hydroxyapatite crystals are known to form mineral deposits on the heart valve surface

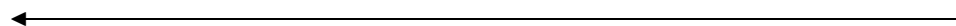


Figure 5. FT-IR spectra of the human heart valves: aortic, mitral, tricuspid and pulmonary. All spectra were normalized using the CH vibrational mode at 1447 cm^{-1} .

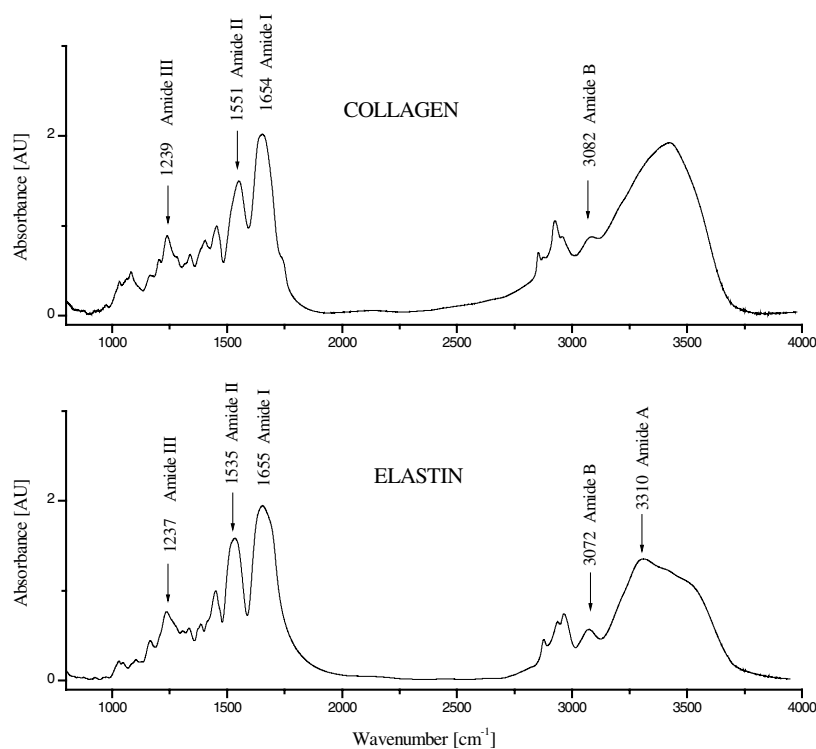


Figure 6. FT-IR spectra of the collagen and elastin.

(Jorge-Herrero et al. 2005). On the other hand, Low-Ying et al. (2002) and Sockalingum et al. (2002) report, that absorption in the range $1000\text{--}1250\text{ cm}^{-1}$ is typical for vibrations of the CH and COH groups from carbohydrates. Polycarbohydrates are the main components of the glycosaminoglycans (GAGs). The GAGs and glycoproteins form the ground substance of the valve tissue.

Conclusions

The AFM working in the contact mode in air is a useful tool for imaging surfaces of human heart valves at the supramolecular level.

In accordance with the layered and complex structure of valve leaflets, the considerable heterogeneity of the surface topography for all valves was observed. AFM images revealed areas with entirely different spatial organization of the collagen fibril bundles. Zones with multidirectional, stacked collagen fibrils, as well as areas with regular dense packing of thin collagen fibrils were found. It was also found that different forms of fibril packing had an impact on the collagen D-spacing distance.

Using AFM method, it was also possible to image objects that correspond to some pathological states of heart valves at their early stages, i.e. mineral deposits locating on the valve surface.

Analysis of the peak frequencies in the IR spectra allowed us to recognize different components, i.e. collagen and elastin, in the layers of the valve leaflets. The ventricularis layer, which is abundant in elastin, and fibrosa layer containing mostly collagen, were spectroscopically recognized. Moreover, carbohydrates and minerals deposits (hydroxyapatites) were detected. Carbohydrates are the main components of GAGs. The presence of mineral deposits was supported by the AFM method.

Our results demonstrate that AFM imaging in the contact mode and FT-IR spectroscopy are suitable methods for structural characterization of heart valves at the molecular and supramolecular levels. Such investigations can be useful for improvements in technology of bioprosthetic valves.

Acknowledgements. Support of the State Committee for Scientific Research, Poland, grant No. NN-2-365/05 is gratefully acknowledged.

References

- Baselt D. R., Revel J. P., Baldeschwieler J. D. (1993): Subfibrillar structure of type I collagen observed by atomic force microscopy. *Biophys. J.* **65**, 2644—2655
- Chang M. C., Tananka J. (2002): FT-IR study for hydroxyapatite/collagen nanocomposite cross-linked by glutaraldehyde. *Biomaterials* **23**, 4811—4818
- Datta D., Kundu P. K., Bandyopadhyay B. N. (1999): Bioprosthetic heart valve – replacing order with chaos: electron microscopic study. *Artif. Organs* **23**, 372—376
- Hurle J. M., Colve E., Fernandez-Teran M. A. (1985): The surface of the human aortic valve as revealed by scanning electron microscopy. *Anat. Embryol.* **172**, 61—67
- Ignjatović N., Savić V., Najman S., Plavšić M., Uskoković D. (2001): A study of HAP/ PLLA composite as a substitute for bone powder, using FT-IR spectroscopy. *Biomaterials* **22**, 571—575
- Jastrzebska M., Barwinski B., Mroz I., Turek A., Zalewska-Rejdak J., Cwalina B. (2005): Atomic force microscopy investigations of chemically stabilized pericardium tissue. *Eur. Phys. J. E, Soft Matter* **16**, 381—388
- Jena B. P., Hörber J. K. (2002): Methods in cell biology. In: *Atomic Force Microscopy in Cell Biology*. Vol. 68, Academic Press
- Jorge-Herrero E., Garcia Paez J. M., Del Castillo-Olivares Ramos J. L. (2005): Tissue heart valve mineralization: review of calcification mechanism and strategies for prevention. *J. Appl. Biomater. Biomech.* **3**, 67—82
- Kunzelman K. S., Cochran R. P., Murphree S. S., Ring W. S., Verrier E. D., Eberhart R. C. (1993): Differential collagen distribution in the mitral valve and its influence on biomechanical behaviour. *J. Heart Valve Dis.* **2**, 236—244
- Low-Ying S., Shaw A., Leroux M., Mantsch H. (2002): Quantitation of glucose and urea in whole blood by mid-infrared spectroscopy of dry film. *Vib. Spectrosc.* **28**, 111—116
- Mirzaie M., Meyer T., Schwartz P., Lotfi S., Rastan A., Schöndube F. (2002): Ultrastructural alterations in acquired aortic and mitral valve disease as revealed by scanning and transmission electron microscopical investigations. *Ann. Thorac. Cardiovasc. Surg.* **8**, 24—30

- Revenko I., Sommer F., Minh D. T., Garrone R., Franc J. M. (1994): Atomic force microscopy study of the collagen fibre structure. *Biol. Cell.* **80**, 67—69
- Rosenthal I. T., Shaw B. W., Hardesty R. L. (1983): Principles of multiple organ procurement from cadaver donors. *Ann. Surg.* **198**, 617—621
- Schoen F. J., Levy R. J. (1999): Tissue heart valves: current challenges and future research perspectives. *J. Biomed. Mater. Res.* **47**, 439—465
- Singh B. R. (2000): *Infrared analysis of peptides and proteins: principles and applications.* American Chemical Society, Washington DC
- Sockalingum G. D., Sandt C., Toubas D., Gomez J., Pina P., Beguinot I., Witthuhn F., Aubert A., Allouch P., Pinon J. M., Manfait M. (2002): FTIR characterisation of *Candida* species: a study on some reference strains and pathogenic *C. albicans* isolated from HIV⁺ patients. *Vib. Spectrosc.* **28**, 137—146
- Stevens A., Lowe J. (1997): *Human Histology.* (2nd ed.), Mosby, Philadelphia
- Twardowski J., Anzenbacher P. (1994): *Raman and IR Spectroscopy in Biology and Biochemistry.* Ellis Horwood, Chichester
- Yacoub M. H., Cohn L. H. (2004): Novel approaches to cardiac valve repair: from structure to function: Part I. *Circulation* **109**, 942—950

Final version accepted: March 23, 2006